Measurement of single top-quark production in the s-channel in proton–proton collisions at $\sqrt{s} = 13\text{TeV}$ with the ATLAS detector

[ATLAS-CONF-2022-030]

LHCTopWG open meeting

Timothée Theveneaux-Pelzer
on behalf of the ATLAS collaboration

Humboldt-Universität zu Berlin

Wednesday June 15$^{\text{th}}$ 2022

European Research Council
Established by the European Commission

Single-top production

- Single-top production : 3 processes at LO in perturbative theory

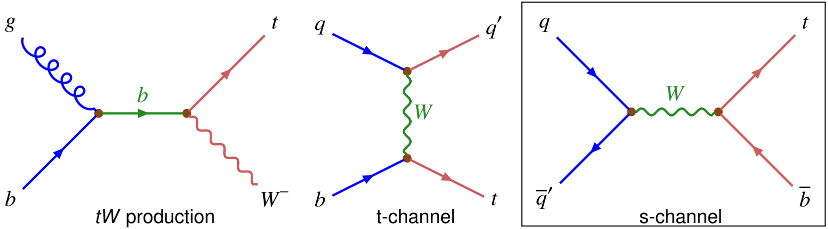

- s-channel : $q\bar{q}$ induced process - the most challenging at the LHC
  - $\rightarrow$ s-channel/$t\bar{t}$ ratio decreases when $\sqrt{s}$ increases : 0.021 at 8 TeV, 0.012 at 13 TeV
- Importance to measure this process at all energies
  - $\rightarrow$ specific sensitivity to new physics - useful for EFTs & anomalous coupl. interpretations

Existing single-top measurements at the LHC

- Latest single-top summary plot :

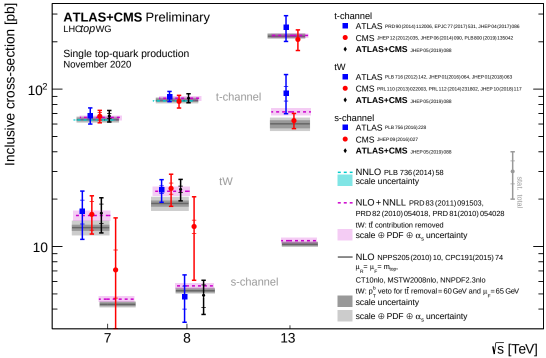

- 8 TeV s-channel cross-section measurements :

ATLAS	$4.8^{+1.8}_{-1.5}$ pb	3.2 σ (3.9 σ exp.)	Phys. Lett. B **756** (2016) 228
CMS	13.4 ± 7.3 pb	2.3 σ (0.8 σ exp.)	JHEP **09** (2016) 027
ATLAS+CMS	4.9 ± 1.4 pb		JHEP **05** (2019) 088

- Process not yet observed in *pp* collisions - no measurement yet at 13 TeV

Analysis overview

- New ATLAS preliminary result at $\sqrt{s} = 13$ TeV - ATLAS-CONF-2022-030
  - → full run-2 dataset : 139 fb^{-1}
- Selection of signal-like events in the single-lepton channel
  - → 1 e or μ + 2 central jets, b-tagged + $E_{\text{T}}^{\text{miss}}$&$m_{\text{T}}(W)$

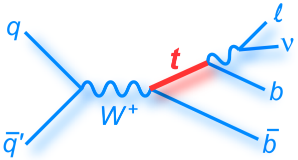

- Signal and backgrounds estimated using MC samples
  - → multijet production modelled with jet-electron and anti-muon methods
- Using Matrix-Element-Method to discriminate signal from backgrounds
  - → same technique used for the ATLAS 8 TeV evidence paper
- Signal cross-section measured with a profile likelihood template fit

MC samples and predicted cross-sections

- Signal and prompt lepton backgrounds modelled with MC samples
- Fake and non-prompt lepton backgrounds modelled with template methods

s-channel	Powheg+Pythia8 (NLO)	$10.32^{+0.40}_{-0.36}$ pb (HATHOR, NLO)
t-channel		217^{+9}_{-8} pb (HATHOR, NLO)
tW		71.7 ± 3.8 pb (Kidonakis, NLO+NNLL)
$t\bar{t}$		832^{+40}_{-46} pb (TOP++, NNLO+NNLL)
$W \to \ell\nu$	Sherpa 2.2.1 (NLO multileg)	60.2 nb (FEWZ, NNLO)
$Z \to \ell^+\ell^-$		6.32 nb (FEWZ, NNLO)
Diboson		cross-section from Sherpa
multijet	Pythia8 (LO)	–

- Dominant backgrounds : $t\bar{t}$ dilepton and $\ell + jets$, W+jets
- Sub-dominant backgrounds : t-channel, multijet
- Smaller backgrounds : tW, Z+jets, Diboson

Events selection

- Events selection targetting signal events topology
  - $\rightarrow$ trigger : lowest unprescaled single e/μ trigger
  - $\rightarrow$ $= 1$ e/μ w. $p_T > 30$ GeV & $|\eta| < 2.47/2.5$
  - $\rightarrow$ ≥ 2 jets w. $p_T > 25$ GeV & $|\eta| < 2.5$
  - $\rightarrow$ $E_T^{miss} > 35$ GeV $m_T(W) > 30$ GeV

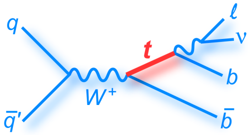

- 4 orthogonal regions :

◇ SR : measurement of the signal cross-section
- $\rightarrow$ $= 2$ jets w. $p_T > 30$ GeV & $|\eta| < 2.5$, leading jet : $p_T > 40$ GeV
- $\rightarrow$ both jets b-tagged with 77% efficiency working point (MV2c10 tagger)
- $\rightarrow$ reject events w. additional leptons w. 10 GeV $< p_T <$ 30 GeV ($t\bar{t}$ veto)
- $\rightarrow$ reject events w. additional jets w. 20 GeV $< p_T <$ 30 GeV or $|\eta| > 2.5$ ($t\bar{t}$, t-chan. veto)

◇ W+jets VR : validation of discriminant shape for W+jets events
- $\rightarrow$ $= 2$ jets w. $p_T > 30$ GeV & $|\eta| < 2.5$
- $\rightarrow$ both jets b-tagged with 85% WP, at least one failing the 77% WP
- $\rightarrow$ reject events w. additional leptons w. 10 GeV $< p_T <$ 30 GeV ($t\bar{t}$ veto)

◇ $t\bar{t}$-jets VR4 : validation of discriminant shape for $t\bar{t}$ events
- $\rightarrow$ $= 4$ jets w. $p_T > 25$ GeV & $|\eta| < 2.5$, $= 2$ b-tagged with 77% WP

◇ $t\bar{t}$-jets VR3 : validation of discriminant shape for $t\bar{t}$ events
- $\rightarrow$ $= 3$ jets w. $p_T > 25$ GeV & $|\eta| < 2.5$, $= 2$ b-tagged with 77% WP

Multijet estimation : jet-electron and anti-muon methods

- Multijet production contaminate selected events due to fake and non-prompt leptons
  - → estimation using template methods (see e.g. ATLAS-CONF-2014-058)
- Jet-electron template to model multijet shapes in the electron channel
  - → jets with large fraction of energy in the EM calorimeter in Pythia8 di-jet MC sample
- Anti-muon template to model multijet shapes in the muon channel
  - → inverting identification and isolation requirements in data
- Fit in fakes-enriched region to estimate the (pre-fit) multijet yields
  - → SR selection, but $E_{\mathrm{T}}^{\mathrm{miss}}$ ($m_{\mathrm{T}}(W)$) cut removed in the electron (muon) channel
  - → $E_{\mathrm{T}}^{\mathrm{miss}}$ ($m_{\mathrm{T}}(W)$) distribution used in the electron (muon) channel to perform the fit
  - → procedure repeated in the three VRs, to get a multijet estimate in these regions
- Multijet uncertainties
  - → normalisation : 30%
  - → shape : variation of template definition parameters

Multijet estimation : $E_{\mathrm{T}}^{\mathrm{miss}}$ and $m_{\mathrm{T}}(W)$ distributions

- Data/MC comparison in both channels, after multijet yield estimation
  - → top : $E_{\mathrm{T}}^{\mathrm{miss}}$ in the e channel ; bottom : $m_{\mathrm{T}}(W)$ in the μ channel
  - → error band : norm. ($W + jets$: 40%, multijet : 30%, top : 6%), shape (multijet), MC stat.

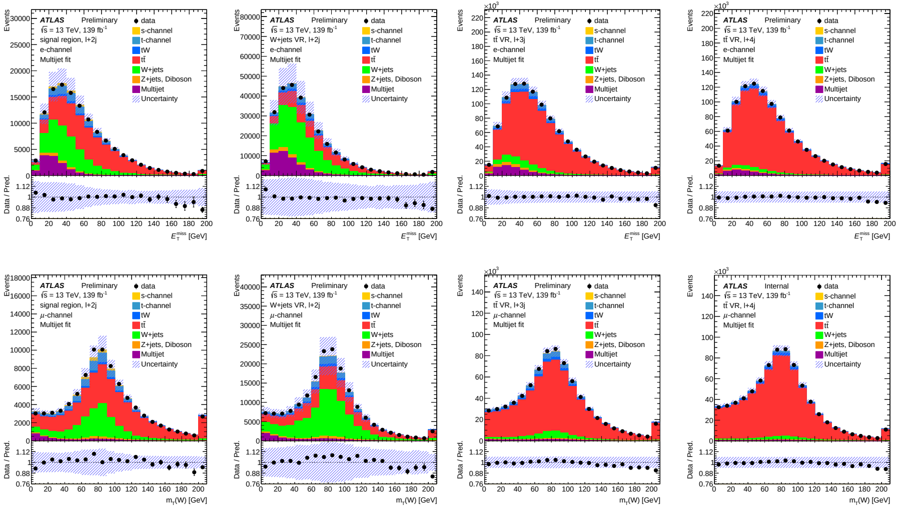

The Matrix Element Method in a (condensed) nutshell

- For each event X calculate likelihood $\mathcal{P}(X\,|\,H_{\mathrm{proc}})$ that the event is of type H_{proc}
  - → X defined by the reco. objects (1 e/μ, 2 b-tagged jets, $E_{\mathrm{T}}^{\mathrm{miss}}$) and their kinematics
  - → H_{proc} represents a process of certain type
- Each likelihood is calculated by :

$$\mathcal{P}(X\,|\,H_{\mathrm{proc}}) = \int \mathrm{d}\Phi \, \frac{1}{\sigma_{H_{\mathrm{proc}}}} \frac{\mathrm{d}\sigma_{H_{\mathrm{proc}}}}{\mathrm{d}\Phi} \, T_{H_{\mathrm{proc}}}(X\,|\,\Phi)$$

  - → Φ : the parton-level state, over which one has to integrate
  - → $\frac{1}{\sigma_{H_{\mathrm{proc}}}} \frac{\mathrm{d}\sigma_{H_{\mathrm{proc}}}}{\mathrm{d}\Phi}$: diff. cross-section, calculated at LO
  - → transfer function $T_{H_{\mathrm{proc}}}(X\,|\,\Phi)$: energy resolutions, efficiencies, and permutations
- 8 processes are calculated, each with at least 1 e/μ, 2 jets, at least 1 ν
  - → s-channel, with 2 or 3 outgoing partons (0 or 1 radiations)
  - → t-channel in the 4FS, $t\bar{t}$ ℓ+jets, $t\bar{t}$ dilepton, $W+bb$, $W+cj$, $W+jj$
- Calculation of discriminant $P(S\,|\,X)$ for each event, using Bayes' theorem

$$P(S\,|\,X) = \frac{\sum_i P(S_i)\,\mathcal{P}(X\,|\,S_i)}{\sum_i P(S_i)\,\mathcal{P}(X\,|\,S_i) + \sum_j P(B_j)\,\mathcal{P}(X\,|\,B_j)}$$

  - → $P(S\,|\,X)$: probability to be a signal event, given its topology X
  - → S_i (B_j) : the 2 (6) signal (background) processes
  - → $P(S_i)$ and $P(B_j)$ calculated using expected fraction for each process

Validation of the MEM discriminant

- Distributions of the discriminant $P(S \mid X)$ in the three VRs to validate the shape
- Error band : normalisation uncertainties and MC statistics

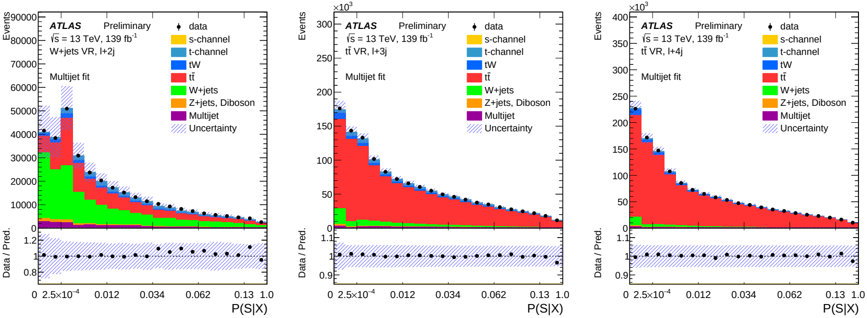

Statistical analysis and systematic uncertainties

- Signal cross-section measured with a profile likelihood fit of $P(S|X)$ in the SR
  - → binning optimised to improved sensitivity while keeping MC stat fluctuations reasonable
  - → events with $P(S|X) < 2.5 \times 10^{-4}$ (background-dominated) are not included in the fit
- Normalisation of two main backgrounds $t\bar{t}$ and $W+$jets is free-floating in the fit
  - → modelling uncertainties on these two processes are shape-only
  - → all other nuisance parameters are constrained by Gaussian terms in the likelihood
- Normalisation uncertainties on other backgrounds
  - → t-channel, tW : 4% and 5% (using predicted cross-sections uncertainties)
  - → Z+jets and diboson : 60% (dominated by 50% on the HF component)
  - → multijet : 30% (comparison with other methods)
- Signal and background MC modelling uncertainties :
  - → top processes ISR/FSR : variations of μ_R, μ_F in the ME, and α_S^{ISR}, α_S^{FSR} in the PS
  - → top processes PDFs : PDF4LHC15 error set
  - → top processes PS & had. : Powheg+Herwig7 vs. Powheg+Pythia8
  - → $t\bar{t}$ resummation : variation of hdamp by a factor 2
  - → $t\bar{t}$ matching : aMC@NLO+Pythia8 vs. Powheg+Pythia8
  - → $t\bar{t}/tW$ interference : Powheg+Pythia8 DS vs. DR
  - → $W+$jets : independent variations of μ_R, μ_F in the ME
  - → multijet : two shape uncertainties
- Experimental uncertainties : JES, JER, JVT, b-tagging, $E_{\mathrm{T}}^{\mathrm{miss}}$, leptons, luminosity

Results

- $t\bar{t}$ and W+jets norm. : $0.81^{+0.13}_{-0.12}$ and $1.37^{+0.35}_{-0.31}$
- Measured s-chanel cross-section :
  $\sigma = 8.2 \pm 0.6\ (\text{stat.})^{+3.4}_{-2.8}\ (\text{syst.})\,\text{pb} = 8.2^{+3.5}_{-2.9}\ (\text{tot.})\,\text{pb}$
- Compatible with SM prediction at NLO :
  $\sigma^{\text{SM}} = 10.32^{+0.40}_{-0.36}\,\text{pb}$
- Significance : 3.3 σ (3.9 σ expected)

Process	Event yield	
	Pre-fit	Post-fit
s-channel	4 200 ± 710	3 700 ± 1 100
t-channel	13 000 ± 2 000	15 000 ± 2 300
tW	3 680 ± 970	4 250 ± 1 100
$t\bar{t}$	76 000 ± 12 000	70 600 ± 4 200
W+jets	21 500 ± 2 900	32 200 ± 5 000
Z+jets, VV	2 400 ± 1 400	2 900 ± 1 600
Multijet	2 150 ± 650	1 700 ± 540
Total	123 000 ± 17 000	130 310 ± 620
Data	130 310	

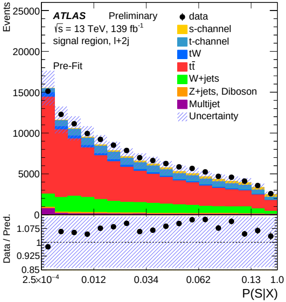

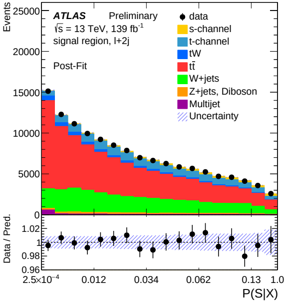

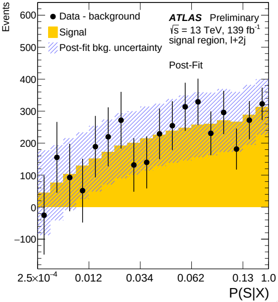

Ranking plot

- Dominant sources :
  - → $t\bar{t}$ normalisation
  - → signal MC modelling
  - → JES, JER
  - → $t\bar{t}$ shape modelling
  - → W+jets normalisation
  - → MC statistics
- All pulls are lower than 1 σ
- $t\bar{t}$ shower and generator shape NPs are midly constrained
  - → typical of 2-point systematics

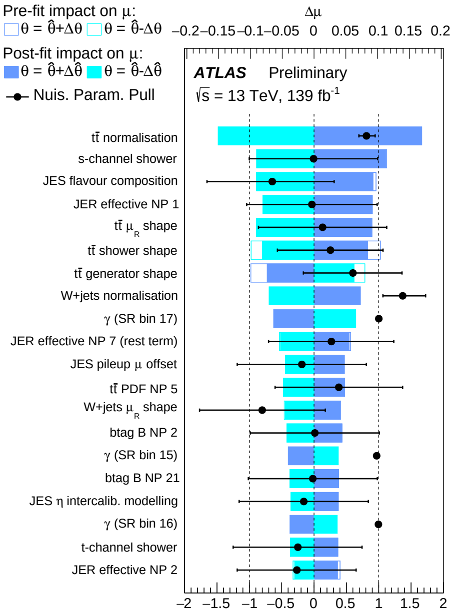

Summary of post-fit impact of uncertainties

Source	$\Delta\sigma/\sigma$ [%]
$t\bar{t}$ normalisation	$+24/-17$
Jet energy resolution	$+18/-12$
Jet energy scale	$+18/-13$
Other s-channel modelling sources	$+18/-8$
Top-quark processes ISR/FSR	$+13/-11$
MC statistics	$+13/-11$
Other $t\bar{t}$ shape modelling sources	$+12/-10$
Flavour tagging	$+12/-10$
W+jets normalisation	$+11/-8$
Top-quark processes PDFs	$+10/-9$
W+jets $\mu_{\mathrm{R}}/\mu_{\mathrm{F}}$ shape	$+6/-5$
Other processes normalisation	$+6/-5$
Pileup	$+5/-3$
Other t-channel modelling sources	± 5
Luminosity	$+4/-3$
Other tW modelling sources	$+1/-2$
Missing transverse energy	± 1
Multijet shape modelling	± 1
Other sources	< 1
Systematic uncertainties	$+42/-34$
Data statistics	± 8
Total	$+42/-35$

Comparison with 8 TeV result

- 8 TeV measurement : Phys. Lett. B **756** (2016) 228

$$\sigma(8\text{ TeV}) = 4.8 \pm 0.8\ (\text{stat.})^{+1.6}_{-1.3}\ (\text{syst.})\,\text{pb}$$
$$= 4.8^{+1.8}_{-1.6}\ (\text{total})\,\text{pb}$$
$$\sigma(13\text{ TeV}) = 8.2 \pm 0.6\ (\text{stat.})^{+3.4}_{-2.8}\ (\text{syst.})\,\text{pb}$$
$$= 8.2^{+3.5}_{-2.9}\ (\text{total})\,\text{pb}$$

- Dominated by systs. in both cases
- Same expected significance : 3.9 σ
  - $\rightarrow$ observed : 3.2(3.3) σ at 8(13) TeV
- S/B : 3.8%(2.9%) at 8(13) TeV

Process	Post-fit yields 8 TeV	Post-fit yields 13 TeV
s-channel	540 ± 160	3700 ± 1100
t-channel	1360 ± 160	15000 ± 2300
tW	380 ± 50	4250 ± 1100
$t\bar{t}$	8100 ± 400	70600 ± 4200
W+jets	3100 ± 500	32200 ± 5000
Z+jets, diboson	410 ± 280	2900 ± 1600
Multijet	800 ± 400	1700 ± 540
Total	14700 ± 180	130310 ± 620
Data	14677	130310

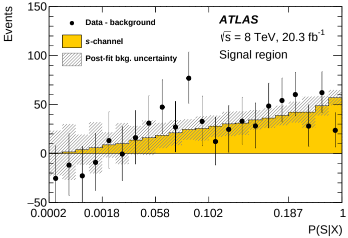

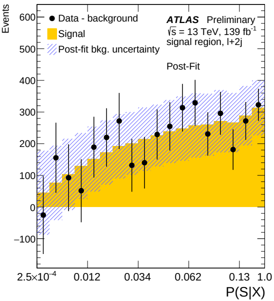

Conclusion

- First measurement of the single-top s-channel cross-section at 13 TeV
  - $\rightarrow$ $\sigma = 8.2 \pm 0.6\ (\text{stat.})^{+3.4}_{-2.8}\ (\text{syst.})\,\text{pb} = 8.2^{+3.5}_{-2.9}\ (\text{total})\,\text{pb}$
  - $\rightarrow$ compatible with SM prediction $\sigma^{\text{SM}} = 10.32^{+0.40}_{-0.36}\,\text{pb}$
- Same expected sensitivity as in the 8 TeV analysis : 3.9 σ
  - $\rightarrow$ observed sensitivity : 3.3 σ at 13 TeV (was 3.2 σ at 8 TeV)

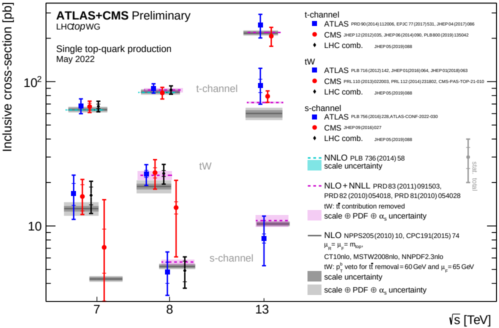

Backup

ATLAS single-top summary plot

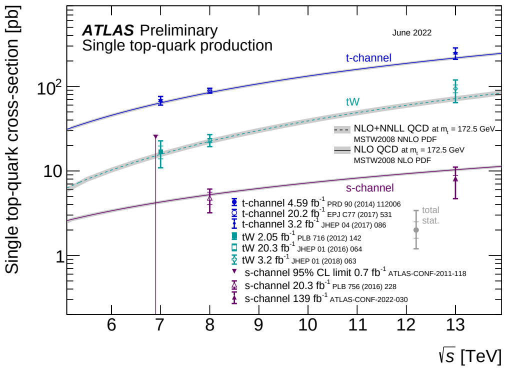

Post-fit Data/MC comparisons

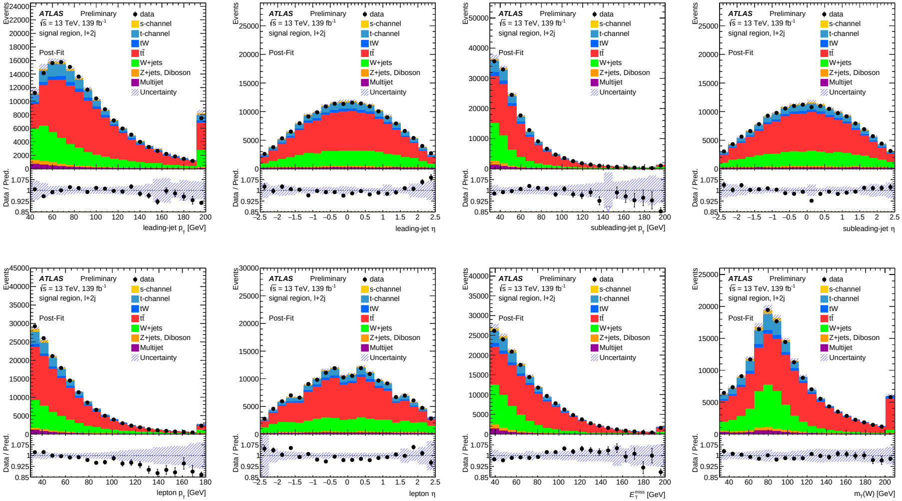

Correlation matrix

ATLAS Preliminary

	JES effective NP modelling 1	JES η intercalib. modelling	JES flavour composition	JES flavour response	JER effective NP 1	JES pileup μ offset	JES pileup ρ topology	btag Light NP 0	multijet normalisation	s-channel shower	$t\bar{t}$ generator shape	$t\bar{t}$ shower shape	$t\bar{t}$ μ_R shape	W+jets μ_R shape	μ	$t\bar{t}$ normalisation	W+jets normalisation
JES effective NP modelling 1	100.0	0.1	0.1	-0.1	-0.4	0.0	-1.5	0.0	0.4	0.6	10.8	6.5	1.7	-5.2	-3.6	13.1	26.8
JES η intercalib. modelling	0.1	100.0	1.6	-0.6	1.2	0.8	0.2	0.4	0.2	0.4	4.2	3.3	0.7	-2.0	13.2	24.0	15.4
JES flavour composition	0.1	1.6	100.0	-1.5	3.1	2.0	0.0	1.2	0.7	1.4	12.5	7.3	2.4	-6.3	32.5	63.7	48.3
JES flavour response	-0.1	-0.6	-1.5	100.0	-1.1	-0.7	-0.2	-0.4	0.1	-0.4	-3.5	-2.8	-0.6	1.5	-11.8	-24.3	-13.5
JER effective NP 1	-0.4	1.2	3.1	-1.1	100.0	1.5	-0.2	1.3	0.2	0.9	3.4	5.9	2.8	-0.4	29.7	30.4	23.5
JES pileup μ offset	0.0	0.8	2.0	-0.7	1.5	100.0	0.3	0.7	0.2	0.5	4.9	4.0	0.9	-2.3	16.3	26.6	23.4
JES pileup ρ topology	-1.5	0.2	0.0	-0.2	-0.2	0.3	100.0	0.2	-1.2	1.6	8.0	3.2	1.9	-3.5	7.8	24.7	16.7
btag Light NP 0	0.0	0.4	1.2	-0.4	1.3	0.7	0.2	100.0	-0.2	0.1	1.1	1.0	0.2	-1.2	11.5	4.2	37.1
multijet normalisation	0.4	0.2	0.7	0.1	0.2	0.2	-1.2	-0.2	100.0	-0.0	-7.4	-5.6	-1.4	-7.9	-10.0	-17.4	22.2
s-channel shower	0.6	0.4	1.4	-0.4	0.9	0.5	1.6	0.1	-0.0	100.0	-2.3	-1.5	-0.7	-1.2	33.1	2.1	2.6
$t\bar{t}$ generator shape	10.8	4.2	12.5	-3.5	3.4	4.9	8.0	1.1	-7.4	-2.3	100.0	-46.6	-9.3	-2.2	-21.6	27.6	13.1
$t\bar{t}$ shower shape	6.5	3.3	7.3	-2.8	5.9	4.0	3.2	1.0	-5.6	-1.5	-46.6	100.0	-4.9	4.9	27.6	27.1	-6.5
$t\bar{t}$ μ_R shape	1.7	0.7	2.4	-0.6	2.8	0.9	1.9	0.2	-1.4	-0.7	-9.3	-4.9	100.0	-0.8	29.6	3.7	0.6
W+jets μ_R shape	-5.2	-2.0	-6.3	1.5	-0.4	-2.3	-3.5	-1.2	-7.9	-1.2	-2.2	4.9	-0.8	100.0	13.7	0.6	-20.2
μ	-3.6	13.2	32.5	-11.8	29.7	16.3	7.8	11.5	-10.0	33.1	-21.6	27.6	29.6	13.7	100.0	54.7	27.0
$t\bar{t}$ normalisation	13.1	24.0	63.7	-24.3	30.4	26.6	24.7	4.2	-17.4	2.1	27.6	27.1	3.7	0.6	54.7	100.0	51.4
W+jets normalisation	26.8	15.4	48.3	-13.5	23.5	23.4	16.7	37.1	22.2	2.6	13.1	-6.5	0.6	-20.2	27.0	51.4	100.0